Contributions of thermal expansion of monuments and nearby bedrock to observed GPS height changes

Haoming Yan,[1,2] Wu Chen,[2] Yaozhong Zhu,[1] Weimin Zhang,[1] and Min Zhong[1]

Received 12 March 2009; revised 13 May 2009; accepted 15 May 2009; published 2 July 2009.

[1] Long-term continuous Global Positioning System (GPS) observations have become an important tool for studying the various geodynamic processes. To fully study the geodynamic processes at GPS stations, the temporal movements of GPS monuments and nearby bedrock induced by thermal expansion need to be considered. In this paper, we extend a theoretical model to estimate the thermal expansions of GPS monuments and nearby bedrock for 86 globally distributed GPS stations based upon measurements of surface air temperatures. The results show that annual temperature variations are the dominant contributors for the thermal expansion of GPS monuments and nearby bedrock. The contributions of thermal expansion to GPS height changes display largely spatial variations and can reach to a few millimeters. **Citation:** Yan, H., W. Chen, Y. Zhu, W. Zhang, and M. Zhong (2009), Contributions of thermal expansion of monuments and nearby bedrock to observed GPS height changes, *Geophys. Res. Lett.*, *36*, L13301, doi:10.1029/2009GL038152.

1. Introduction

[2] Continuous space geodetic observations (e.g., Global Positioning System (GPS), etc.) have become important tools for investigating various geodynamic problems. For example, the time series of global station coordinates provide a unifying framework for deformation monitoring from global to regional scales. The global and regional networks have been used for global reference frame establishment [*Altamimi et al.*, 2002], deformation monitoring for global tectonic plate movement [*Prawirodirdjo and Bock*, 2004], local motion caused by earthquakes and volcanoes [*Bock et al.*, 1993; *Geist et al.*, 2006], and various temporal variations from postglacial rebound [*Johansson et al.*, 2002; *Larson and van Dam*, 2000] to seasonal deformation [*van Dam and Wahr*, 1987; *van Dam et al.*, 1994; *Dong et al.*, 2002].

[3] As the precision in the height coordinate approaches to millimeter level, numerous perturbations other than random noise have to be removed from the coordinate time series. One of these perturbations is the movement of the GPS monuments themselves, which serve the purpose of connecting the surveying equipment to the Earth. The monument movement resulting from various processes, such as, soil swelling in response to rainfall, rock and soil weathering effects, etc. [*Wyatt et al.*, 1989; *Beavan*, 2005], may be divided into two processes. The first process is random movement of a monument, known as monument noise. The second process is the monument movement caused by thermal expansion due to temperature changes, or caused by soil compaction, etc. Monument noise may be characterized by certain statistical processes, e.g., the random walk or Gauss-Markov processes, through the analysis of long-term GPS position residuals [*Beavan*, 2005; *Williams et al.*, 2004]. Although it is difficult to identify the exact statistical process that controls monument noise, it has been shown that GPS data noise quality varies between different monument types [*Williams et al.*, 2004; *Langbein*, 2008]. Thermal expansion of a monument, on the other hand, can cause the horizontal and vertical movements. *Prawirodirdjo et al.* [2006] show that a large part of the annual variations in the horizontal position time series of Southern California Integrated GPS stations, can be explained by thermoelastic strain in the elastic part of the Earth's crust induced by atmospheric temperature variations. And the vertical movement effects had previously been studied by *Dong et al.* [2002] and *Romagnoli et al.* [2003]. *Romagnoli et al.* [2003] use a linear thermal expansion model to estimate the thermal expansion effect on GPS height changes for both a steel pole on the ground and concrete pillar under the ground. To account for temperature differences between the surface and soil at depth, a simple scaling factor of 4 is adopted to convert surface temperature to soil temperature. *Dong et al.* [2002] present a theoretical heat conduction model to model the nearby bedrock thermal expansion effect on GPS height changes. They give a qualitative conclusion that the amplitude of the annual height changes induced by bedrock thermal expansion is approximately 0.5 mm or less and with a 45° phase delay following the surface temperature.

[4] In this paper, we present a generalized model of thermal expansion that can account for the vertical motion of GPS antennas. This model has two components; the first being the thermal expansion of the component of the monuments located above ground, and the second being the thermal expansion of the ground's surface through heat conduction [e.g., *Dong et al.*, 2002] into nearby bedrock. Instead of only considering the annual temperature change component in the *Dong et al.* [2002] study, our model will provide a more general solution to include the entire frequency spectrum of surface temperature changes. Using this model, we calculate the bedrock thermal effect on a global scale based on the global surface air temperature time series from the National Centers for Environmental Prediction/National Center for Atmospheric Research (NCEP/NCAR) reanalysis. The results show that the amplitudes of the bedrock thermal effect vary as with a location. The largest

[1]Key Laboratory of Dynamic Geodesy, Institute of Geodesy and Geophysics, Chinese Academy of Sciences, Wuhan, China.
[2]Department of Land Surveying and Geo-Informatics, Hong Kong Polytechnic University, Hong Kong, China.

0094-8276/09/2009GL038152

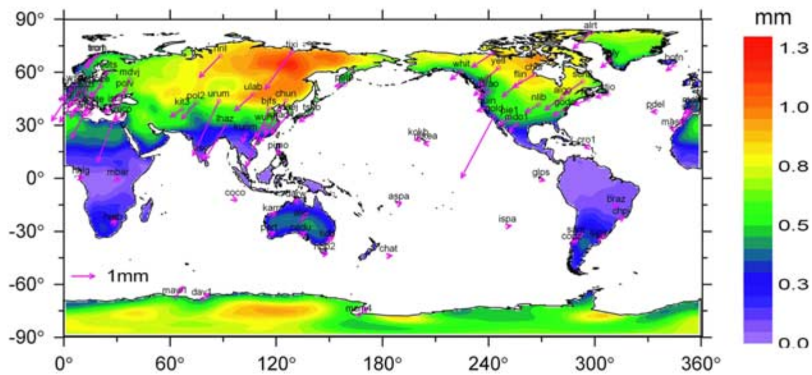

Figure 1. Annual amplitudes of bedrock thermal vertical displacements as determined from the model (contours) and annual thermal vertical displacement vectors for the 86 IGS stations. The vector amplitude A and phase φ are defined as $A\sin(\omega(t - t_0) + \varphi)$. Where t_0 is 1999.0 and ω is the annual circular frequency. The vector lengths represent the amplitudes. The phases are counted counterclockwise from the east.

amplitude of annual height change induced by bedrock thermal expansion can reach approximately 1.3 mm, which is 2.6 times larger than that presented by *Dong et al.* [2002]. To verify this model, we have compared the model predictions with the GPS observations from 86 globally distributed International GNSS (Global Navigation Satellite System) Service (IGS) stations. The results show that by adding the thermal expansion corrections, the predicted station movements are better fitted with the observational GPS data.

2. Monument Thermal Expansion Model

[5] High quality GPS monuments generally consist of two parts: an underground foundation physically attaching the monument to the bedrock and supporting structures above the ground to where the actual GPS antenna is fixed. To quantify monument thermal expansion due to surface temperature changes, it is important to determine the temperature distribution within the monument. In this paper, we use surface air temperature data to approximately quantify the thermal effects on the supporting structures above the ground, and use a classical heat conduction equation to estimate the temperature distribution of the bedrock.

[6] The supporting structures of monuments are commonly metal rods with concrete pillars, which can extend up to several meters above the ground. Assuming the temperature of the supporting materials has the same temperature as the surface air temperature measured at the station, the thermal expansion of the supporting structures (or concrete pillar) can be determined by

$$\Delta L = \alpha \cdot L \cdot \Delta T \qquad (1)$$

where ΔL is the length change in meters, α is the linear thermal expansion coefficient, and $\alpha = 12 \times 10^{-6}$ (1/°C) for the concrete pillar, L is the supporting structures length in meters, and ΔT is the temperature change in Celsius degrees relative to a reference point.

[7] The thermal expansion model for bedrock applied here was derived from *Dong et al.* [2002], but with an extension to include the entire frequency spectrum of surface temperature variability. The vertical displacements $\Delta h(t)$ of the surface due to bedrock thermal effects are:

$$\Delta h(t) = \frac{1+\nu}{1-\nu}\alpha \sum_{i=1}^{N} A_i \sqrt{\frac{\kappa}{\omega_i}} \cos\left(\omega_i t - \frac{\pi}{4} - \varphi_i\right) \qquad (2)$$

where ν is the Poisson's ratio, κ is the thermal diffusivity which is independent of depth and time (for common rock material, κ is 1 mm^2/s [e.g., *Dong et al.*, 2002]), N is the number of harmonics, and A_i, ω_i and φ_i are the amplitudes, circular frequency, and initial phase of the ith harmonic of surface temperature, respectively.

[8] From Equation (2) we can see there is a gain factor $\frac{1+\nu}{1-\nu}$, which takes the thermal stress into account when calculating the vertical displacements. Assuming, for example, that ν is 0.25 (the typical ν for concrete and steel is 0.20 and 0.27–0.30, respectively), this gain is about 1.7. Also, the phase of vertical displacements of Equation (2) has a 45° delay following the surface temperature changes.

3. Results

[9] To examine the applicability of the model described in Section 2, we first calculate the thermal expansion using Equation (2) on the global scale, and then compared the model predictions with the observed GPS height changes for 86 globally distributed IGS stations using Equations (1) and (2).

3.1. Thermal Expansion of Global Continents and IGS Stations

[10] To obtain the thermal expansion changes of the bedrock, we used a least squares fit method to get seasonal (annual and semiannual) harmonics from the global daily surface air temperature time series obtained from the NCEP/NCAR reanalysis (http://www.cdc.noaa.gov/). Using these seasonal air temperature harmonics and Equation (2), the seasonal vertical displacements of bedrock can be calculated. The annual amplitudes for the vertical displacements of bedrock are approximately proportional with latitude; the higher the latitude, the larger the vertical displacements (Figure 1, contours). The largest variations are in North

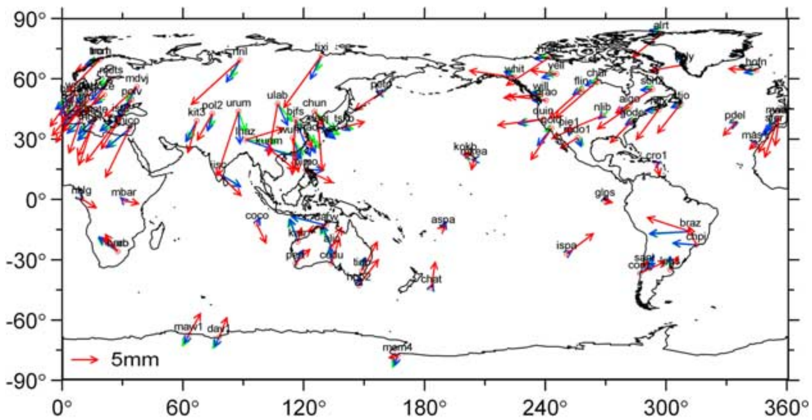

Figure 2. Comparison of annual vertical displacements among the mass contributions (green vectors), the summations of thermal model predictions and mass contributions (blue vectors), and the observed GPS height changes (red vectors) for the 86 IGS stations. The amplitudes and phases are defined the same way as in Figure 1.

Asia, North America, and the Antarctic. In these regions, the annual amplitudes of bedrock vertical displacements are all significantly larger than 0.5 mm; especially in North Asia, where it can reach 1.3 mm, which is 2.6 times larger than the prediction of *Dong et al.* [2002]. The semiannual amplitudes of bedrock vertical displacements (not shown) are less than 20% of the corresponding annual term on the global continents, and can be neglected.

[11] The diurnal surface temperature changes are also a dominant component in surface air temperature variations. As the diurnal surface air temperature changes can only affect the upper bedrock temperature changes, the thermal expansion of bedrock caused by diurnal surface air temperature changes has little influence on the GPS height changes (less than 0.015 mm) and can be neglected.

3.2. Comparison Between Model Predictions and Observed GPS Height Changes

[12] The 86 IGS reference stations are used to verify our model in this study (see Figure 1 and Table S1 for details).[1] The observed daily GPS heights used here are created by a Scripps Orbit and Permanent Array Center (SOPAC) refined model [*Nikolaidis*, 2002] that takes into account offsets, linear velocity, and annual and semi-annual fluctuations (available at http://sopac.ucsd.edu). The time span of the 86 IGS stations height time series is 2∼8 years from January 1999 to December 2006 (see Table S1 for details). The above ground components for the installation of GPS antennas are obtained from IGS stations log files (available at http://igscb.jpl.nasa.gov, also in Table S1). The daily surface air temperature changes of the 86 IGS stations are interpolated from the NCEP/NCAR gridded surface air temperatures.

[13] Using Equations (1) and (2), we model the thermal vertical displacements at the 86 IGS stations. Then the annual amplitude and phase (shown in Figure 1) are estimated using a least squares fit with the following expression:

$$y_t = b_0 + b_1 t + A\sin(\omega(t - t_0) + \varphi) + \varepsilon_t \tag{3}$$

where y_t is the displacement time series, A is the amplitude and ω is the annual circular frequency, φ is the phase (reference date for the phase is Jan. 1, 1999), b_0 and b_1 are the nominal displacement and rate, and ε_t is the random noise.

[14] The amplitudes of annual thermal vertical displacements are significant in the regions of latitude greater than 25°N (denoted by Region A hereafter, total 57 stations) and the Antarctic, but negligible in the other regions (Figure 1, vectors). In Region A, there are 21 stations with the annual thermal vertical displacements greater than 1.0 mm, 9 stations greater than 1.5 mm and 6 stations greater than 2.0 mm (Table S2). The annual phases of thermal vertical displacements on Region A are approximately 225°. The maximum annual thermal vertical displacement is 3.9 mm at MDVJ station in the 86 IGS stations.

[15] Except for the vertical displacements induced by the thermal expansion, the observed GPS height changes are also influenced by other loading effects [*Dong et al.*, 2002], e.g., mass loading contributions of atmosphere, ocean bottom pressure (OBP) and hydrology. In this study, we use the NCEP/NCAR surface pressure [*Kalnay et al.*, 1996], Estimating the Circulation and Climate of the Ocean (ECCO) OBP (http://ecco.jpl.nasa.gov, version kf066b) and the National Oceanic and Atmospheric Administration (NOAA) Climate Prediction Center (CPC) soil moisture data from http://www.cdc.noaa.gov/ [*Fan and van den Dool*, 2004] to calculate the vertical deformations induced by surface loadings using the Green function method [*Farrell*, 1972; *van Dam and Wahr*, 1987]. Note that the vertical displacements induced by mass loading may vary largely by using different mass loading data sources. Our mass loading results presented here only taken as a reference to compare the thermal contributions to the vertical displacements with the GPS height changes. The annual amplitudes and phases for mass loading contributions (denoted by M hereafter) to the stations height changes are presented in Figure 2 (green vectors). Meanwhile, we also show the annual vectors of summation of the thermal expansion predictions and mass loading contributions (denoted by M + T hereafter, blue vectors), and of the observed GPS height changes (red vectors) in Figure 2, respectively.

[1]Auxiliary materials are available in the HTML. doi:10.1029/2009GL038152.

[16] After considering the thermal expansion contributions, the M + T predictions have a better agreement with the observed GPS height changes in both amplitude and phase angle for the 86 IGS stations (Figure 2, also Figure S1 for a clearer picture). For example, the M + T model predictions agree significantly better with the observed GPS height changes at stations GOLD, URUM, SHAO, BJFS, MDVJ, WSRT, and METS, etc. At the above stations, the thermal effects contribute nearly half of the signals observed in the GPS annual variations, and have larger contributions than the mass loading contributions. The mean annual amplitude ratio of (M + T)/GPS and M/GPS are 60% and 53% respectively, for the 86 IGS stations. This indicates that the thermal contributions can averagely explain 7% annual amplitude of the GPS height changes. Meanwhile, the annual phase of M + T is closer to the GPS height changes by an average of 5-degree than that of M. There is only one station LHAZ, which has the obvious opposite contribution, after considering the thermal effect. The reason for this opposite contribution may need further study.

[17] Furthermore, to assess the presence of the M and the M + T signals in the GPS height changes, we compare the variance of the GPS height residuals before and after applying the M or M + T corrections. The results show that 0%∼65% (or 0%∼45%) of the residuals variances are reduced for 91% (or 90%) of the GPS stations after applying the M + T (or M) corrections (Figure S2). In other words, both M + T and M contributions are found obviously in the GPS height changes. And as we have expected, after considering the thermal expansion contributions, the variance reductions of GPS height residuals are larger than that of only considering the M corrections. There are also variance increase at a few of GPS stations (Figure S2), which can be interpreted as either (1) random or systematic correlation between GPS height errors and errors in M + T or M, or (2) the M + T or M signal is actually larger than GPS height changes.

[18] Although there are better agreements between M + T and the GPS observations, there are still obvious differences on annual variations between the model predictions and the GPS observations (Figure 2). One possible reason for the differences may be due to unmodeled or mis-modeled geophysical signals, especially the hydrological contributions. Though we can use CPC hydrological data to calculate the hydrological contributions to vertical displacements, the shortage of the surface and ground water data used in the CPC model can cause certain extent of uncertainties to vertical displacements.

4. Conclusion and Discussion

[19] In this study, we extend the thermal expansion model of *Dong et al.* [2002] to predict the thermal effects on observed GPS stations height changes. This model can be used successfully together with the mass loading model to better explain the observed annual GPS height changes, especially in higher latitude GPS stations and the stations with GPS antennas installed on a taller monument.

[20] The thermal expansion model accuracy may be affected by many factors. First, the coefficients used in the model are material related. For example, the Poisson's ratio is 0.2 for concrete, 0.3–0.45 for clay, and 0.2 for sand. Thus, the gain factor $\frac{1+\nu}{1-\nu}$ can range from 1.5 to 2.6 for different materials. Also, the linear thermal expansion coefficient varies with different materials, and the accurate measurement of monument height above ground of the GPS antenna is probably a bigger factor. In Equation (2), we take the thermal diffusivity as a constant, but it actually changes with depth and time [*de Silans et al.*, 1996]. The model simplifies an underground structure as a uniform elastic medium without any other effects such as pore pressure, and flow, etc., though their influences are small in most cases. Finally, for the monuments exposed to the sun, the surface air temperature used in this study is different from the ground temperature. This difference causes a small model error. Despite these issues, the model presented in this paper is a good approximation needed to correct GPS height changes due to thermal expansion. When only considering the heat conduction effect of surface air temperature, the nearby bedrock temperature decreases as an exponential function, and only the upper nearby bedrock temperature can significantly affect monument height change. Most GPS antennas are installed on a concrete foundation in the upper bedrock, and the constant values of Poisson's ratio, the linear thermal expansion coefficient, and the thermal diffusivity adopted in this paper are suitable to estimate the GPS height changes induced by thermal expansion.

[21] Understanding seasonal variations of GPS height changes are important for geophysical studies. *Dong et al.* [2002] estimate that less than half of the observed GPS seasonal changes can be explained by the redistribution of geophysical fluid mass loads. Much of the residual variations are probably caused by the GPS errors and unmodeled contributions. For example, *Penna and Stewart* [2003] have demonstrated unmodeled tidal signals can be aliased to longer periods. *Kedar et al.* [2003] show the high-order ionospheric effects on GPS positioning have strong semi-annual characteristics with the peaks at the equinoxes (around March and September) at low latitudes. Recently, *Ray et al.* [2008] extract harmonics with a 351 day period from GPS observations which can be related to the GPS constellation repeat cycle. In this paper, we show that the annual amplitude of the thermal vertical displacement can reach to 3.9 mm, which is significantly larger than the prediction from *Dong et al.* [2002]. Therefore, the thermal effects due to local temperature variations on GPS observations need to be carefully corrected in an analysis of seasonal geophysical signals.

[22] **Acknowledgments.** We would like to thank the editors F. Florindo, E. Calais, and J. Langbein and one anonymous reviewer for their insightful review comments, which improved the presentation of the results. This research is supported by research projects of the National Natural Science Foundation of China, grants 40874049, 40574035, and 40474010, by "863" Program of China, grants: 2006AA09Z153 and 2006AA12Z128, and by HK Polytechnic University Research Funds G-U410 and G-U304.

References

Altamimi, Z., P. Sillard, and C. Boucher (2002), ITRF2000: A new release of the international terrestrial reference frame for earth science applications, *J. Geophys. Res.*, *107*(B10), 2214, doi:10.1029/2001JB000561.

Beavan, J. (2005), Noise properties of continuous GPS data from concrete pillar geodetic monuments in New Zealand and comparison with data from U. S. deep drilled braced monuments, *J. Geophys. Res.*, *110*, B08410, doi:10.1029/2005JB003642.

Bock, Y., et al. (1993), Detection of crustal deformation from Landers earthquake sequence using continuous geodetic measurements, *Nature*, *361*, 337–340.

de Silans, A. M. B. P., B. A. Monteny, and J. P. Lhomme (1996), Apparent soil thermal diffusivity, a case study: HAPEX-Sahel experiment, *Agric For. Meteorol*, *81*, 201–216.

Dong, D., P. Fang, Y. Bock, M. K. Cheng, and S. Miyazaki (2002), Anatomy of apparent seasonal variations from GPS-derived site position time series, *J. Geophys. Res.*, *107*(B4), 2075, doi:10.1029/2001JB000573.

Fan, Y., and H. van den Dool (2004), Climate Prediction Center global monthly soil moisture data set at 0.5° resolution for 1948 to present, *J. Geophys. Res.*, *109*, D10102, doi:10.1029/2003JD004345.

Farrell, W. E. (1972), Deformation of the Earth by surface loads, *Rev. Geophys.*, *10*, 761–797.

Geist, D., W. Chadwick, and D. Johnson (2006), Results from new GPS and gravity monitoring networks at Fernandina and Sierra Negra volcanoes, Galapagos, 2000–2002, *J. Volcanol. Geotherm. Res.*, *150*, 79–97.

Johansson, J. M., et al. (2002), Continuous GPS measurements of postglacial adjustment in Fennoscandia: 1. Geodetic results, *J. Geophys. Res.*, *107*(B8), 2157, doi:10.1029/2001JB000400.

Kalnay, E., et al. (1996), The NCEP/NCAR 40-year reanalysis project, *Bull. Am. Meteorol. Soc.*, *77*, 437–447.

Kedar, S., G. A. Hajj, B. D. Wilson, and M. B. Heflin (2003), The effect of the second order GPS ionospheric correction on receiver positions, *Geophys. Res. Lett.*, *30*(16), 1829, doi:10.1029/2003GL017639.

Langbein, J. (2008), Noise in GPS displacement measurements from southern California and southern Nevada, *J. Geophys. Res.*, *113*, B05405, doi:10.1029/2007JB005247.

Larson, K. M., and T. van Dam (2000), Measuring postglacial rebound with GPS and absolute gravity, *Geophys. Res. Lett.*, *27*, 3925–3928.

Nikolaidis, R. (2002), Observation of geodetic and seismic deformation with the Global Positioning System, Ph.D. thesis, Univ. of California, San Diego.

Penna, N. T., and M. P. Stewart (2003), Aliased tidal signatures in continuous GPS height time series, *Geophys. Res. Lett.*, *30*(23), 2184, doi:10.1029/2003GL018828.

Prawirodirdjo, L., and Y. Bock (2004), Instantaneous global plate motion model from 12 years of continuous GPS observations, *J. Geophys. Res.*, *109*, B08405, doi:10.1029/2003JB002944.

Prawirodirdjo, L., Y. Ben-Zion, and Y. Bock (2006), Observation and modeling of thermoelastic strain in Southern California Integrated GPS Network daily position time series, *J. Geophys. Res.*, *111*, B02408, doi:10.1029/2005JB003716.

Ray, J., Z. Altamimi, X. Collilieux, and T. van Dam (2008), Anomalous harmonics in the spectra of GPS position estimates, *GPS Solution*, *12*, 55–64, doi:10.1007/s10291-007-0067-7.

Romagnoli, C., et al. (2003), Influence of soil consolidation and thermal expansion effects on height and gravity variations, *J. Geodyn.*, *35*, 521–539.

van Dam, T. M., and J. Wahr (1987), Displacements of the Earth's surface due to atmospheric loading: Effects on gravity and baseline measurements, *J. Geophys. Res.*, *92*, 1282–1286.

van Dam, T. M., G. Blewitt, and M. B. Heflin (1994), Atmospheric pressure loading effects on Global Positioning System coordinate determinations, *J. Geophys. Res.*, *99*, 23,939–23,950.

Williams, S. D. P., Y. Bock, P. Fang, P. Jamason, R. M. Nikolaidis, L. Prawirodirdjo, M. Miller, and D. J. Johnson (2004), Error analysis of continuous GPS position time series, *J. Geophys. Res.*, *109*, B03412, doi:10.1029/2003JB002741.

Wyatt, F. K., H. Bolton, S. Bralla, and D. C. Agnew (1989), New designs of geodetic monuments for use with GPS, *Eos Trans. AGU*, *70*, 1054.

W. Chen, Department of Land Surveying and Geo-Informatics, Hong Kong Polytechnic University, Hung Hom, Kowloon, Hong Kong, China.

H. Yan, W. Zhang, M. Zhong, and Y. Zhu, Key Laboratory of Dynamic Geodesy, Institute of Geodesy and Geophysics, Chinese Academy of Sciences, Wuhan 430077, China. (yhm@asch.whigg.ac.cn)